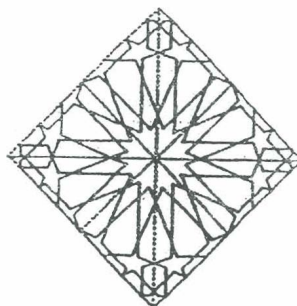




AEIC' 93

AL-AZHAR ENGINEERING THIRD
INTERNATIONAL CONFERENCE
December 18-21 1993



FACULTY OF ENGINEERING
AL - AZHAR UNIVERSITY
NASR CITY , CAIRO, EGYPT

VOLUME (5)
ELECTRICAL ENGINEERING
Electrical Power and Machines

	Page
PROFILES OF FLUX LINES TRAJECTORIES IN THE VICINITY OF HYBRID AC/DC TRANSMISSION LINES Mohamed M. AboElsaad and Mousa A. Abd-Allah	387
THRUST DERATING DUE TO STABILITY REQUIREMENTS OF THE ZIGZAG LINEAR SYNCHRONOUS MOTOR-PAIR INTEGRATING LIFT AND THRUST FOR MAGLEY VEHICLES S. M. Al-Kasimi and M. J. M. Alawi	396
COMPUTATION OF EDDY-CURRENT LOSS IN TRANSFORMER WINDINGS A. A. Dahab	407
A NEW BEARINGLESS TRAPIZOIDAL-PASSIVE-ROTOR SYNCHRONOUS MACHINE S. M. Al-Kasimi	419
THRUST DERATING DUE TO STABILITY REQUIREMENTS OF THE TRAPIZOIDAL LINEAR SYNCHRONOUS MOTOR-PAIR INTEGRATING LIFT AND THRUST FOR MAGLEY VEHICLES S. M. Al-Kasimi	427
THE ACCELERATION CHARACTERISTICS OF A PAIR OF TRAPIZOIDAL LINEAR SYNCHRONOUS MOTORS AS COMPARED TO A ZIGZAG PAIR VERSION FOR MAGLEY APPLICATION S. M. Al-Kasimi	435
A COMPARISON BETWEEN OPTIMUM AND NATURAL SAMPLED PWM SWITCHING TECHNIQUES G. Hashem, J. Richardson, S. A. Kandil, and A. A. Sayyar	446
POTENTIAL AND ELECTRIC FIELD DISTRIBUTION ALONG THE INTERFACE OF GIS SPACER M. S. M. Rizk, S. M. El-Safty, A. Nosseir, M. Awad	455
EFFECT OF SPHERICAL VOIDS WITHIN INSULATION STRUCTURES ON THE ELECTRIC FIELD DISTRIBUTION H. M. Ismail	467
ELECTRODE SURFACE ROUGHNESS INITIATED BREAKDOWN IN COMPRESSED SF6 GIS Sayed A. Ward	479

EXPERIMENTAL STUDY OF I
BREAKDOWN IN NON-UNIFC
M. A. Abd-Allah, M. S. M. Rizk

A CHARGE SIMULATION MO
WITHIN SOLID DIELECTRIC/
H. M. Ismail

PREDICTION OF STEADY TI
RATING FOR A WATER CO
Sanaa A. M. Shehata

STUDIES ON THE NEW INS
El-Sayed M. El-Refaie

ANALYTICAL AND EXPERIM
EFFECT OF THE SOIL MOI
CHARACTERISTICS OF UN
Fatma A Mohamed

THE PERFORMANCE OF TH
ASSOCIATED WITH AUTOI
G. M. A. El-Salam, A. A. Atia

MICROPROCESSOR-BASE
MULTIPLE RELAYS
S. M. W. Ahmed

EVALUATION&REDUCTIO
PARTIAL&COMPLETE FAI
CORRECTION CAPACITO
DISTRIBUTION SYSTEM V
Mohamed A. A. Wahab A.
Khalil

DETECTION METHOD BA
QUANTITIES IN HV RADII
M. M. M. Mahmud

PREFOMANCE EVALUN
ALGORITHMS
M. M. Mansour, K. M. El-N



AEIC'93

AL-AZHAR ENGINEERING THIRD
INTERNATIONAL CONFERENCE
DECEMBER 18-21, 1993



المؤتمر العلمي الدولي الثالث
تحت المظلة - جامعة الأزهر
من ١٨ إلى ٢١ ديسمبر ١٩٩٣ م

**THRUST DERATING DUE TO STABILITY REQUIREMENTS OF THE
ZIGZAG LINEAR SYNCHRONOUS MOTOR-PAIR INTEGRATING
LIFT AND THRUST FOR MAGLEV VEHICLES**

S. M. Al-Kasimi* and M. J. M. Alawi**

* Assistant prof., Electrical and Computer Eng. Dept.,
Umm-Ul-Qura University, P.O.Box 6112, Makka, Saudi Arabia.

** Graduate Assistant, Electrical and Computer Eng. Dept.,
Umm-Ul-Qura University, Saudi Arabia.

ABSTRACT

The Zigzag Linear Synchronous Motor Pair, ZLSMP, is composed of two magnets one of which is shown in Fig.1. These are attached to the maglev vehicle-bogie as shown in Fig.2, and are reacting against the zigzag-shaped rail shown in Fig.3. The coils of each magnet are connected as shown in Fig.4, with dc coils fed from a chopper power amplifier controlling field current to provide lift at constant gap, Z . The feedback loops involved in field control are shown in Fig.5. The ac are, on the other hand, fed from a two-phase inverter providing armature currents such that the field is distorted among the four sub-poles of each magnet, and hence propulsion is obtained.

It was found necessary to make a twin pair of magnets, for the elimination of harmonic currents in the field circuits. This also improves the thrust force pulsation. Maximum thrust force was found when the armature mmf rms value equals to that of field mmf. This maximum thrust force relative to supported weight was found to be $\pi Z/p$, where p is the pole-pitch shown in

The work described in the proposed paper looks upon the stability requirements of ZLSMP and proves that the above maximum thrust value corresponds to un-lift system. To make it controllable, this maximum thrusting force must be severely derated to gain

KEYWORDS

Zigzag; linear; synchronous; motor; magnetic suspension.

INTRODUCTION

The Zigzag Linear Synchronous Motor Pair, one of which is shown in Fig.1. These are attached to the maglev vehicle-bogie as shown in Fig.2, and are reacting against the zigzag-shaped rail shown in Fig.3. As the rail moves relative to magnets in the field, emf's will appear at sub-pole coil terminals for constructive emf resultant, ac coils are connected in series and are fed from a two-phase inverter providing armature currents such that the field current to provide lift at constant gap, Z . The feedback loops involved in field control are shown in Fig.5. The inverter providing armature currents such that the field is distorted among the four sub-poles of each magnet and hence propulsion is obtained.

West [1] found it necessary to make a twin pair of magnets, for the elimination of harmonic currents in the field circuit. This also improves the thrust force pulsation. Maximum thrust force was found when the armature mmf rms value equals to that of field mmf. This maximum thrust force relative to the supported weight was found to be $\pi Z/p$, where p is the pole-pitch shown in Fig.3.

This paper reviews the theory of ZLSMP and proves that the above maximum thrusting force must be derated for stability.

NOTATIONS

The symbols used in this paper are listed below

- A sub-pole surface area
- A_i overlap area of sub-pole i in motor-A
- α derated maximum thrust relative to weight
- B_i flux density over sub-pole i in motor-A
- E_i open circuit induced voltage at phase i coil
- F_h horizontal force of both motor pairs
- F_v vertical lift force of both motor pairs



المؤتمر العلمي الدولي الثالث
لبنية الهندسة - جامعة الازهر
من ٨ رجب ١٤١٤ هـ
من ١٨ إلى ٢١ ديسمبر ١٩٩٣ م

STABILITY REQUIREMENTS OF THE ZIGZAG MOTOR-PAIR INTEGRATING FOR MAGLEV VEHICLES

and M. J. M. Alawi**
Electrical and Computer Eng. Dept.,
P.O. Box 6112, Makka, Saudi Arabia.
Electrical and Computer Eng. Dept.,
King Fahd University, Saudi Arabia.

The Zigzag Linear Synchronous Motor Pair, ZLSMP, is composed of two magnets, one of which is shown in Fig.1. These are attached to the maglev vehicle-boggye as shown in Fig.2, and are reacting against the zigzag-shaped rail shown in Fig.3. As the rail moves relative to magnets in the direction indicated in Fig.3, induced emf's will appear at sub-pole coil terminals due to the field excitation. Hence, for constructive and resultant, ac coils are connected as shown in Fig.4. The dc coils are connected in series and are fed from a chopper power amplifier controlling the field current to provide lift at constant gap, Z . The feed-back loops involved in the field control are shown in Fig.5. The ac coils are fed from a two-phase inverter providing armature currents such that the field is distorted among the four sub-poles of each magnet, and hence propulsion is obtained.

West [1] found it necessary to make a twin pair of magnets for the elimination of harmonic currents in the field circuit. This also cancels the thrust force pulsation, leaving only a steady component which he found to have a maximum when the sub-polar armature mmf rms value equals to that of field. This maximum thrust relative to the supported weight was found to be $\pi Z/p$, where p is the pole-pitch shown in Fig.3.

This paper reviews the theory of ZLSMP and then looks at its stability requirements. It then proves that the above maximum thrust value corresponds to an uncontrollable lift system. To make it controllable, this maximum thrusting force must be derated for stability.

KEYWORDS

Zigzag; linear; synchronous; motor; machine; thrust; derating; maglev; vehicle; suspension.

INTRODUCTION

The Zigzag Linear Synchronous Motor Pair, ZLSMP, is composed of two magnets, one of which is shown in Fig.1. These are attached to the maglev vehicle boggye as shown in Fig.2, and are reacting against the zigzag shaped rail shown in Fig.3. As the rail moves relative to magnets in the direction indicated in Fig.3, induced emf's will appear at sub-pole coil terminals due to the field excitation. Hence, for constructive and resultant, ac coils are connected as shown in Fig.4. The dc coils are connected in series and are fed from a chopper power amplifier controlling the field current to provide lift at constant gap, Z . The feed-back loops involved in the field control are shown in Fig.5. The ac coils are fed from a two-phase inverter providing armature currents such that the field is distorted among the four sub-poles of each magnet and hence propulsion is obtained.

West [1] found it necessary to make a twin pair of magnets for the elimination of harmonic currents in the field circuit. This also cancels the thrust force pulsation, leaving only a steady component which he found to have a maximum when the sub-polar armature mmf rms value equals to that of field. This maximum thrust relative to the supported weight was found to be $\pi Z/p$, where p is the pole-pitch shown in Fig.3.

This paper reviews the theory of ZLSMP and then looks at its stability requirements. It then proves that the above maximum thrust value corresponds to an uncontrollable lift system. To make it controllable, this maximum thrusting force must be derated for stability.

NOTATIONS

The symbols used in this paper are listed below:

- A sub-pole surface area
- A_i overlap area of sub-pole i in motor-A
- α derated maximum thrust relative to weight
- B_i flux density over sub-pole i in motor-A
- E_i open circuit induced voltages phase i coil terminals in motor-A
- F_h horizontal thrust force of both motor pairs
- F_v vertical lift force of both motor pairs

- ϕ_{ii} flux due to m_i which leaves sub-pole i of motor-A
- ϕ_{ij} flux due to m_i which leaves sub-pole i to sub-pole j of motor-A
- ϕ_k flux due to all sub-polar mmfs that leaves sub-pole k in motor-A
- I_D current flowing in the field dc coils
- i_i current flowing in phase- i ac coils
- M_D net dc mmf excitation of field winding per pole in motor-A
- \bar{M}_D optimum M_D value for maximum thrust
- m peak value of ac mmf excitation of any phase per sub-pole
- \bar{m} optimum m value for maximum thrust
- m_i ac mmf excitation of phase- i armature winding per sub-pole
- m_j resultant mmf excitation around sub-pole j of motor-A
- μ_0 permeability of air
- N number of turns of ac coil around any sub-pole
- N_D number of turns of dc coil around any pole
- p pole-pitch
- τ perturbation level of m_1 relative to operational level of M_D
- T time period to complete one cycle
- t time, starting zero when rail completely links sub-poles 1 and 3 of motor-A
- θ phase angle of ac excitation of motor-A
- $\bar{\theta}$ optimum phase angle at maximum thrust conditions
- θ_m optimum phase angle at derated maximum thrust conditions
- u speed of rail relative to magnet
- W weight of supported boggie
- ω angular frequency of ac supply
- Z energized air gap

ASSUMPTIONS

For simplicity, the following assumptions were made:

1. All sub-poles have the same surface area.
2. AC coils around sub-poles are identical.
3. Slot-width in the main poles, fringing, leakage flux, friction and other drag forces are all neglected.
4. Air gap, Z , is homogeneous over the surface.
5. Flux lines in the energized airgaps are perpendicular to the magnet pole-surface.
6. The energized air-gap faces equal areas at the magnet pole-surface below it through the air gap.
7. The energized area per pole is composed of two adjacent sub-poles with flux density varying sinusoidally between zero and A .
8. Speed of motor relative to the track, u , is constant.
9. Track structure is rigid.
10. Reference axes are taken to be the ground axes perpendicular to both.
11. The motor does not rotate about any of its poles.
12. The motor force is considered in two directions: perpendicular to the direction of motion and along the direction of motion. In the third direction is exerted, it will be ignored.
13. Flux linkage for any ac coil varies sinusoidally when its sub-pole is fully uncoupled to the rail and fully coupled to the rail.
14. The induced voltages in all ac coils around a sub-pole are equal.
15. AC coils are fed with sinusoidal ac current.

MAGNETIC SUB-POLAR EXCITATION

Each of the sub-poles in Fig.4 could be considered as a combination of:

- dc due to the field current I_D flowing in the field coils
- ac due to the ac excitation magnitude of:

$$M_D = N_D$$

ASSUMPTIONS

For simplicity, the following assumptions were made in the analysis to come.

1. All sub-poles have the same surface area, A .
2. AC coils around sub-poles are identical.
3. Slot-width in the main poles, fringing, leakage, steel loss, copper loss, windage, friction and other drag forces are all negligible.
4. Air gap, Z , is homogeneous over the sub-poles.
5. Flux lines in the energized airgaps are parallel.
6. The energized air-gap faces equal areas both at the rail-surface above it and at the magnet pole-surface below it throughout the motion.
7. The energized area per pole is composed of two portions. Each portion belongs to one of the two adjacent sub-poles within the main pole and is assumed to vary sinusoidally between zero and A .
8. Speed of motor relative to the track, u , is constant.
9. Track structure is rigid.
10. Reference axes are taken to be the gravity line, motion line and the axis perpendicular to both.
11. The motor does not rotate about any of the above axes.
12. The motor force is considered in two directions only, namely, along the gravity line and along the direction of motion. Although some force component in the third direction is exerted, it will be ignored.
13. Flux linkage for any ac coil varies sinusoidally between a minimum of zero when its sub-pole is fully uncoupled to the rail and a maximum when its sub-pole is fully coupled to the rail.
14. The induced voltages in all ac coils around sub-poles vary sinusoidally.
15. AC coils are fed with sinusoidal ac currents phase-locked to rail.

MAGNETIC SUB-POLAR EXCITATIONS FOR MOTOR-A

Each of the sub-poles in Fig.4 could be considered excited with two components:

- dc due to the field current I_D flowing in the dc coil of N_D turns, thus giving a dc excitation magnitude of:

$$M_D = N_D I_D, \quad (1)$$

and:

- ac due to the armature phase currents i_A or i_B flowing in the ae coils of N turns each, thus giving an ac excitation magnitude of:

$$m_A(t) = N i_A(t) = m \cos(\omega t + \theta), \quad (2)$$

or:

$$m_B(t) = N i_B(t) = m \sin(\omega t + \theta); \quad (3)$$

where: $\omega = 2\pi/T$, with $T = 2p/u$; hence: $w = \pi u/p$.

Using Fig.4 and denoting m_1, m_2, m_3 and m_4 to be the resultant mmf excitations around sub-poles 1, 2, 3 and 4 respectively of motor-A, with positive sense when forcing flux to leave the sub-pole, then:

$$m_1(t) = -M_D - m_A(t) = -m_3(t), \quad (4)$$

and:

$$m_2(t) = -M_D + m_A(t) = -m_4(t). \quad (5)$$

ENERGIZED SUB-POLAR AREAS FOR MOTOR-A

With A_1, A_2, A_3 and A_4 defined as above, then these areas are assumed sinusoids between a maximum of A and a minimum of zero. The equations describing these approximations are given by:

$$A_1(t) = A_3(t) = (A/2) [1 + \cos(\omega t)], \quad (6)$$

and:

$$A_2(t) = A_4(t) = (A/2) [1 - \cos(\omega t)]. \quad (7)$$

MAGNETIC SUB-POLAR FLUXES FOR MOTOR-A

Let $\phi_{11}, \phi_{12}, \phi_{13}, \phi_{14}, \phi_{21}, \phi_{22}, \phi_{23}, \phi_{24}, \phi_{31}, \phi_{32}, \phi_{33}, \phi_{34}, \phi_{41}, \phi_{42}, \phi_{43}, \phi_{44}, \phi_1, \phi_2, \phi_3$ and ϕ_4 be as defined earlier. Hence, each of m_1, m_2, m_3 and m_4 mmfs is driving an associated magnetic circuit similar to that shown in Fig.6. Hence, using Fig.6 and applying superposition, the fluxes $\phi_1(t), \phi_2(t), \phi_3(t)$ and $\phi_4(t)$ leaving sub-poles 1, 2, 3 and 4 of motor-A respectively due to all mmfs of m_1, m_2, m_3 and m_4 are found to be:

$$\phi_1(t) = \phi_{11} - \phi_{21} - \phi_{31} - \phi_{41} = \mu_0 A_1 m_1/Z, \quad (8)$$

$$\phi_2(t) = \mu_0 A_2 m_2/Z, \quad (9)$$

$$\phi_3(t) = -\phi_1(t), \quad (10)$$

and:

$$\phi_4(t) = -\phi_2(t). \quad (11)$$

This gives the sub-polar flux densities as.

$$B_1(t) = \mu$$

$$B_2(t) = \mu$$

$$B_3(t) = -$$

and:

$$B_4(t) = -$$

MAGNETIC LIFT FORCE FOR ZI

Motor-A will exert a lift force, F_{v_A} , in or mizing the energized air-gap, Z . This lift is given by:

$$F_{v_A}(t) = \sum_{i=1}^4$$

Using eqs.(6) and (7) for A_1, A_2, A_3 and B_2, B_3 and B_4 respectively; and simplifying and m_B ; then F_{v_A} may be found as:

$$F_{v_A}(t) = \mu_0 A [M_D^2 + m_A^2]$$

Motor-F will exert a lift force, F_{v_B} , which

$$= \mu_0 A [M_D^2 + m_B^2]$$

Hence, the total lift force, F_v , of ZLSMP

$$F_v(t) = F_{v_A}(t) + F_{v_B}(t) = \mu_0 A [2$$

which is seen to be steady to support via field control. The pulsating component implicit in both expressions of F_{v_A} and F_{v_B} connections of both motor pairs. Hence, for stable field excitation, $M_D(\theta, m)$, at as:

$$W = \mu_0 A [2 M_D^2 + m^2]$$

OPEN CIRCUIT VOLTAGES FOR

The open circuit induced voltage, E_A , at Fig.4 to be:

$$E_A(t) = N \frac{d}{dt} [\phi_2 -$$

ats i_A or i_B flowing in the ac coils of N ion magnitude of:

$$i_A = m \cos(\omega t + \theta), \quad (2)$$

$$i_B = m \sin(\omega t + \theta); \quad (3)$$

$$\text{hence: } \omega = \pi u/p.$$

Let m_A to be the resultant mmf excitations of motor-A, with positive sense when

$$m_A(t) = -m_3(t), \quad (4)$$

$$m_A(t) = -m_4(t). \quad (5)$$

AREAS FOR MOTORS

Let the areas be assumed sinusoidal and of zero. The equations describing these

$$A_1 = (A/2) [1 + \cos(\omega t)], \quad (6)$$

$$A_2 = (A/2) [1 - \cos(\omega t)]. \quad (7)$$

FLUXES FOR MOTOR-A

Let $\phi_{31}, \phi_{32}, \phi_{33}, \phi_{34}, \phi_{41}, \phi_{42}, \phi_{43}, \phi_{44}$ be the fluxes, each of m_1, m_2, m_3 and m_4 mmfs is similar to that shown in Fig.6. Hence, using fluxes $\phi_1(t), \phi_2(t), \phi_3(t)$ and $\phi_4(t)$ leaving respectively due to all mmfs of m_1, m_2, m_3 and

$$\phi_{31} - \phi_{41} = \mu_0 A_1 m_1/Z, \quad (8)$$

$$\mu_0 A_2 m_2/Z, \quad (9)$$

$$= -\phi_1(t), \quad (10)$$

$$= -\phi_2(t). \quad (11)$$

This gives the sub-polar flux densities as:

$$B_1(t) = \mu_0 m_1/Z, \quad (12)$$

$$B_2(t) = \mu_0 m_2/Z, \quad (13)$$

$$B_3(t) = -B_1(t), \quad (14)$$

$$B_4(t) = -B_2(t). \quad (15)$$

and:

MAGNETIC LIFT FORCE FOR ZLSMP

Motor-A will exert a lift force, F_{vA} , in order to minimize its reluctance by minimizing the energized air-gap, Z . This lift force is composed of several parts and is given by:

$$F_{vA}(t) = \sum_{i=1}^4 \frac{A_i B_i^2}{2 \mu_0}$$

Using eqs.(6) and (7) for A_1, A_2, A_3 and A_4 ; eqs.(12), (13), (14) and (15) for B_1, B_2, B_3 and B_4 respectively; and simplifying with the aid of eqs.(2) and (3) for m_A and m_B ; then F_{vA} may be found as:

$$F_{vA}(t) = \mu_0 A [M_D^2 + m_A^2 + 2 M_D m_A \cos(\omega t)]/Z^2. \quad (16)$$

Motor-B will exert a lift force, F_{vB} , which can be similarly found to be:

$$F_{vB}(t) = \mu_0 A [M_D^2 + m_B^2 + 2 M_D m_B \sin(\omega t)]/Z^2. \quad (17)$$

Hence, the total lift force, F_v , of ZLSMP is given as:

$$F_v(t) = F_{vA}(t) + F_{vB}(t) = \mu_0 A [2 M_D^2 + m^2 + 2 M_D m \cos(\theta)]/Z^2, \quad (18)$$

which is seen to be steady to support the boggie weight, W , at constant gap via field control. The pulsating component at twice the synchronous frequency implicit in both expressions of F_{vA} and F_{vB} has been cancelled due to the clever connections of both motor pairs. Hence, the above equation gives the condition for stable field excitation, $M_D(\theta, m)$, at any ac excitation parameters of θ and m as:

$$W = \mu_0 A [2 M_D^2 + m^2 + 2 M_D m \cos(\theta)]/Z^2. \quad (19)$$

OPEN CIRCUIT VOLTAGES FOR ZLSMP

The open circuit induced voltage, E_A , at phase-A coil terminals can be seen from Fig.4 to be:

$$E_A(t) = N \frac{d}{dt} [\phi_2 - \phi_1 + \phi_3 - \phi_4]_{m=0}.$$

This is found to be:

$$E_A(t) = -2N \mu_0 M_D A \omega \sin(\omega t) / Z. \quad (20)$$

Similarly, E_B can be found to be:

$$E_B(t) = 2N \mu_0 M_D A \omega \cos(\omega t) / Z. \quad (21)$$

MAGNETIC THRUST FORCE FOR ZLSMP

The **ZLSMP thrust** force, F_h , can be obtained using the energy principle. Assuming ideal conversion, then, the mechanical power is equated to the electrical power and hence:

$$F_h u = E_A i_A + E_B i_B.$$

This is found to be:

$$F_h(t) = 2 \mu_0 \pi A M_D m \sin(\theta) / p / Z. \quad (22)$$

Hence; the thrust force, F_h , is composed of only one steady component. The α second harmonic component of motor-A cancelled that of motor-B due to the clever connection of **both motors**.

Eq.(22) shows that the ZLSMP will propel when the current phase angle is within $(0, \pi)$ and brake within $(\pi, 2\pi)$. This is due to the mechanical and electrical system lags. The ZLSMP can be used either for motoring with electric power converted to kinetic power or for braking with kinetic power converted to electric. At two θ values, namely: 0 and π , the ZLSMP is exerting virtually zero force.

MAXIMUM THRUST OF ZLSMP

The maximum of $F_h(\theta, m)$ for a given θ occurs at $\bar{m}(\theta)$. This could be found using eqs.(19) and (22) to give:

$$\bar{M}_D(\theta) = \bar{m}(\theta) / \sqrt{2}; \quad (23)$$

where:

$$\bar{m}(\theta) = Z \sqrt{\frac{W}{\mu_0 A [2 + \sqrt{2} \cos(\theta)]}}. \quad (24)$$

On the other hand, the maximum of $F_h(\theta)$ occurs at $\bar{\theta}$. This could be found using eqs.(19) and (22) to be:

$$\bar{\theta} = \pm 135^\circ. \quad (25)$$

This gives the following maximum thrust:

$$F_{h_{max}} = \pi W Z / p.$$

Substituting either $\bar{\theta}$ values in eqs.(23) and (24)

$$\bar{m} = Z \sqrt{\frac{2W}{\mu_0 A}}$$

and:

$$\bar{M}_D = Z \sqrt{\frac{W}{\mu_0}}$$

STABILITY OF ZLSMP LIFT SYSTEM

The ZLSMP lift system shown in Fig.5 is controlled. These signals are:

1. the gap, Z , that can be measured using the motor poles,
2. the gap speed, Z^* , that can be measured in a certain frequency band, and;
3. the pole flux linkage, λ , that can be measured using magnet poles.

Since the equations of the ZLSMP lift system are nonlinear, linearization techniques are used to avoid extreme instability; Linear Control Theory is utilized to design a feedback signals. The controller is shown in Fig.6. The circuit that adds up all three signals after appropriate scaling with the pre-determined characteristics.

The ZLSMP lift-system being considered for stability analysis. The variables perturbing about a non-zero operating point must be much smaller than the magnitude of the perturbation. If these two conditions are violated, the linearization of the actual system. This will consequently cause instability.

The most critical variable in this respect was typically given as:

$$m_1(t) = -M_D -$$

This suggests that the perturbation in $m_1(t)$ is proportional to the level of M_D . Using eq.(2), the ratio r of the perturbation level of M_D is found as:

$$r = m/M_D$$

which at maximum thrusting force indicated is:

$$r = \sqrt{2}.$$

$$f_D A \omega \sin(\omega t) / Z.$$

$$D A \omega \cos(\omega t) / Z.$$

R ZLSMP

ined using the energy principle. Assum-
power is equated to the electrical power

$$4 + E_B i_B.$$

$$D m \sin(\theta) / p / Z.$$

l of only one steady component. The
A cancelled that of motor-B due to the

. when the current phase angle is within
to the mechanical and electrical system
motoring with electric power converted
c power converted to electric. At two
erting virtually zero force.

urs at $\bar{m}(\theta)$. This could be found using

$$(\theta) / \sqrt{2};$$

$$\frac{W}{1 + \sqrt{2} \cos(\theta)}$$

occurs at $\bar{\theta}$. This could be found using

$$15^\circ.$$

$$r Z / p.$$

Substituting either $\bar{\theta}$ values in eqs.(23) and (24) for \bar{m} & \bar{M}_D gives:

$$\bar{m} = Z \sqrt{\frac{2W}{\mu_0 A}},$$

and:

$$\bar{M}_D = Z \sqrt{\frac{W}{\mu_0 A}}.$$

STABILITY OF ZLSMP LIFT SYSTEM

The ZLSMP lift system shown in Fig.5 is controlled using three feed-back signals. These signals are:

1. the gap, Z, that can be measured using the capacitance between the rail and motor poles,
2. the gap speed, Z', that can be measured using differentiation of Z over a certain frequency band, and:
3. the pole flux linkage, λ, that can be measured using a search coil around the magnet poles.

Since the equations of the ZLSMP lift system are nonlinear with inherited extreme instability; linearization techniques are applied to obtain a linearized model, whereby Linear Control Theory is utilized to design a controller using the above feed-back signals. The controller is shown in Fig.5 and is composed simply of a circuit that adds up all three signals after appropriate scaling so that the resulting system complies with the pre-determined characteristics.

The ZLSMP lift-system being considered for linearization is trusted to have each of its variables perturbing about a non-zero operational level. Moreover, the magnitude of perturbation must be much smaller than the operational level. If either of these two conditions is violated, the linearized model is no longer representative to the actual system. This will consequently endanger stability.

The most critical variable in this respect was found to be the sub-polar mmf, typically given as:

$$m_1(t) = -M_D - m_A(t).$$

This suggests that the perturbation in $m_1(t)$ is equal to $m_A(t)$ plus the perturbation of M_D . Using eq.(2), the ratio r of the perturbation of $m_1(t)$ to the operating level of M_D is found as:

$$r = m / M_D;$$

which at maximum thrusting force indicated in eq.(23) evaluates to:

$$r = \sqrt{2}.$$

This violates both conditions trusted to the lift system. To correct for that, \bar{m} must be derated to match reasonable level for r . Hence, substituting in eq.(22):

$$F_h = 2\mu_0 \pi A r M_D^2 \sin(\theta) / p Z.$$

But M_D relates to W using eq.(19) as:

$$M_D^2 = \frac{W Z^2}{\mu_0 A [2 + r^2 + 2r \cos(\theta)]}.$$

Hence:

$$F_h(\theta) = \frac{2\pi r W Z \sin(\theta)}{p [2 + r^2 + 2r \cos(\theta)]}$$

This is maximum at θ_m given by:

$$\theta_m = \cos^{-1} \left(\frac{-2r}{2 + r^2} \right).$$

The resulting thrust force is:

$$F_{h_{max}}(r) = \frac{2\pi r W Z}{p \sqrt{4 + r^2}}.$$

Hence, derated maximum thrust relative to weight is:

$$\alpha = \frac{2r}{\sqrt{4 + r^2}} (\pi Z / p).$$

For the linearized lift model to represent the actual ZLSMP lift system, the value of r must be fairly small. Hence:

$$\alpha \cong r (\pi Z / p).$$

This shows that the maximum thrust relative to weight is derated by factor r from its value at passive support due to active lift of ZLSMP weight. Tolerable perturbation level depends on the severity of nonlinearity of ZLSMP relationships, and could reach as low as 10 % of the operational level. This results in a 10 % derating α from its due when ZLSMP is passively supported.

CONCLUSION

This paper shows that the representability of the linearized model used to design a controller for stable active suspension of ZLSMP system, is derating the maximum thrust of the ZLSMP that can be achieved when passively supported, say by wheels. Suspending ZLSMP actively using the controller shown in Fig.5 has the price of derating the maximum thrust from its value when supported otherwise. The derating factor equals the acceptable level of perturbation relative to the operational level of sub-polar mmf excitation. This can be as bad as 10 %.

REFERENCES

- [1] West, A. N. (1982). The Zigzag Linear Homopolar Synchronous Motor. PhD. Thesis, Elect. Eng. Dept., Manchester University.

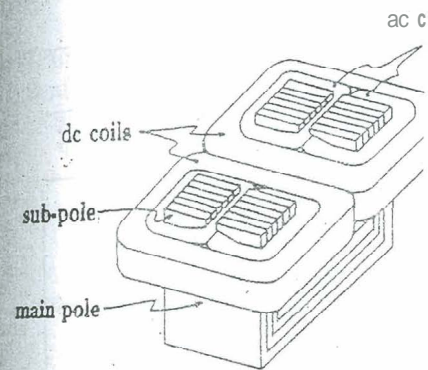


Fig.1 Magnet

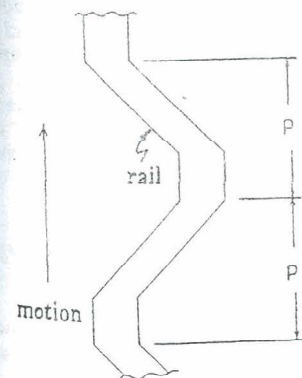
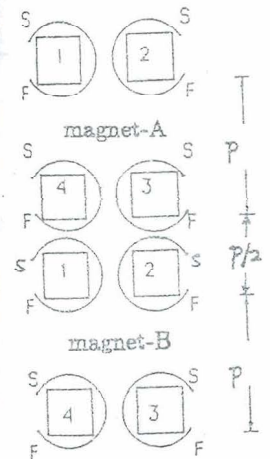


Fig.3 Rail

at system. To correct for that, ... Hence, substituting in eq.(22) ... $v(\theta)/p/Z$.

$$\frac{2r \cos(\theta)}{1 + r^2}$$

$$\frac{\sin(\theta)}{1 + r^2}$$

$$\frac{2r}{-r^2}$$

$$\frac{WZ}{1 + r^2}$$

weight is:

$$Z/p$$

actual ZLSMP lift system, the value

$/p$.

tive to weight is derated by factor ... tive lift of ZLSMP weight. Tolerable f nonlinearity of ZLSMP relationships ... rational level. This results in a 10% passively supported.

of the linearized model used to design ... ZLSMP system, requires derating the ... be achieved when passively supported ... ely using the controller shown in Fig. ... thrust from its value when supported ... acceptable level of perturbation relative ... excitation. This can be as bad as 10%.

ar Homopolar Synchronous Mot ... er University.

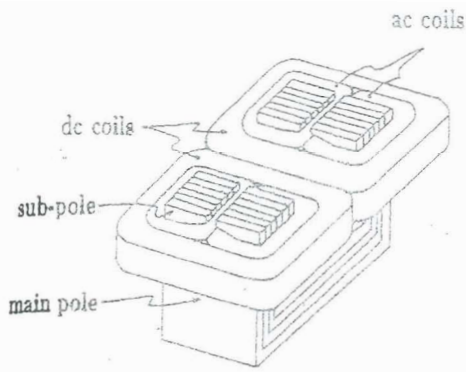


Fig.1 Magnet

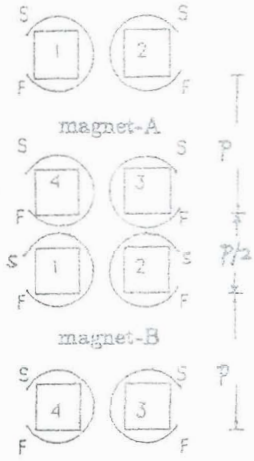


Fig.3 Rail

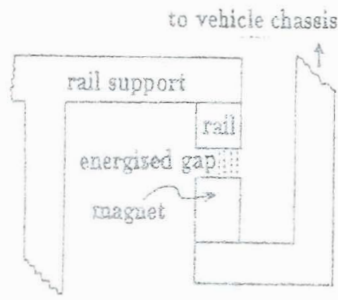


Fig.2 Boggie support

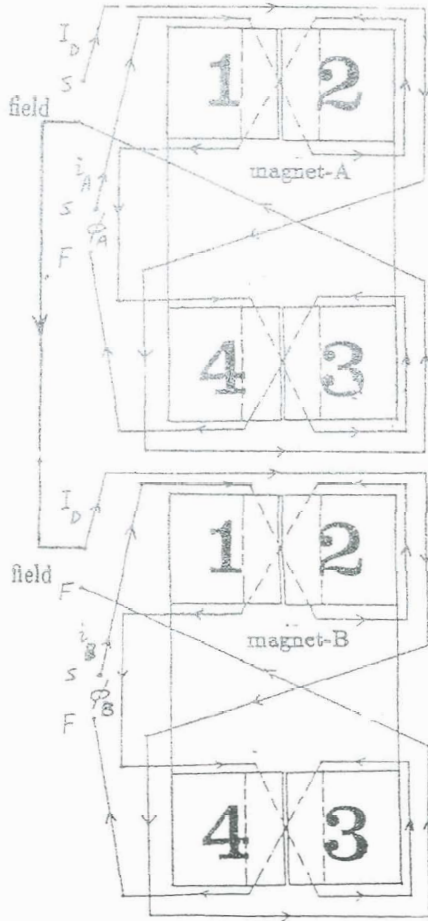


Fig.4 Coil connections

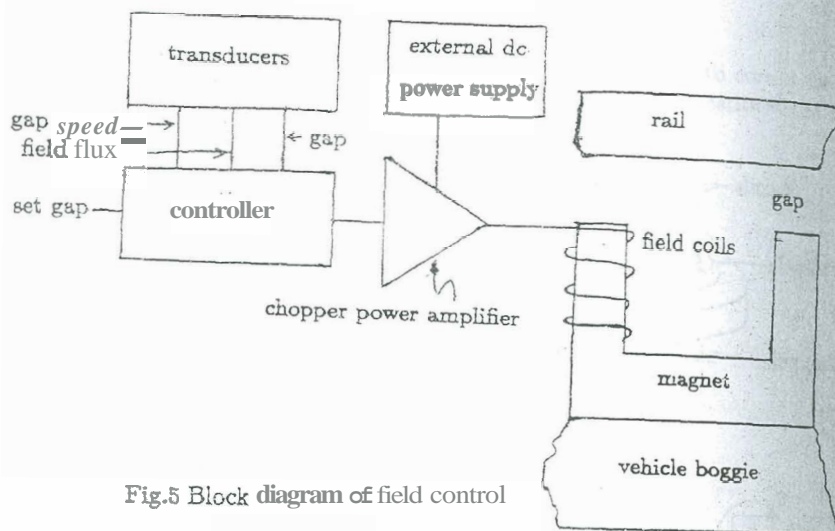


Fig.5 Block diagram of field control

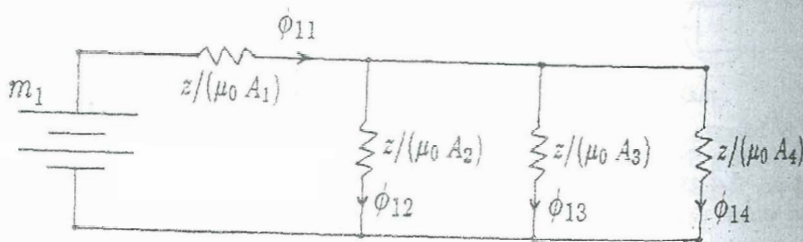


Fig.6 Magnetic circuit driven by m_1 around sub-pole 1

A. A
Dept. of El
Faculty
Menoufi
Sheb:

ABSTRACT

The calculation of eddy-current factor in the design of power transformers make every effort to reduce the calculation and loss of loss calculation and loss proposed to compute eddy-current. The method is based on the distribution of a transformer. is accounted for by means of currents. The validity and is demonstrated by applying cases. The test cases include distribution transformer by Egypt and a core-type transformer air-cored reactors. The those obtained by a static. The method is simple and and reactors the designer so he can to

KEYWORDS

Power transformers, eddy-current, electromagnetic field theory